Optica Applicata, Vol. XV, No. 4, 1985

Variable wavelength interferometry I. Fringe-field method for transmitted light*

Maksymilian Pluta

Central Optical Laboratory, ul. Kamionkowska 18, 03–805 Warszawa, Poland.

A new interferometric technique has been developed for measuring the optical path difference over the entire visible spectrum. The technique depends on using monochromatic light with continuously variable wavelength. One of the basic advantages of this technique is a simple procedure of identifying the interference order in case of large optical path differences. This new method is especially recommended when used together with the Biolar PI double-refracting interference microscope which enables the wavelength of monochromatic light to be measured in real time.

1. Introduction

The main task of interferometry of any kind is to determine correctly the interference order in the image of the object under study. This task may be simplified significantly by using a new interferometric method. This method, using the monochromatic light of continuously variable wavelength, will be called shortly VAWI.

The idea of this method has been reported in 1983 in a conference communication [1], but only recently it has been verified experimentally in a broad range of applications. The procedure is somewhat reverse to that applied in the well-known FECO method. The latter is used mainly in systems of multiple-beam interferometry, since only then the interference fringes of equal chromatic orders are narrow sufficiently to attribute relatively accurate light wavelengths. Moreover, a spectrometer or spectrograph is usually installed behind the FECO interference setup, while in the VAWI method a monochromator is placed in front of the interference system. In both the methods, however, the directly measured parameter is the light wavelength.

In order to experimentally verify the VAWI method an interference microscope developed by the author many years ago [2, 3] and produced by the Polish Optical Works in Warsaw was used. Now this microscope is named Biolar PI; it offers the important possibility of measuring currently the wavelength of the monochromatic light.

---

* This work was carried out on the Research Project PR–3.20.

2. Principle of the VAWI method

Let a transparent object be placed in the object plane of the light transmitting interferometer, for example, a stripe of a thin dielectric layer deposited on a glass plate. It is assumed that this object as well as its surrounding medium are characterized by typical runs of the refractive index spectral dispersion (Fig. 1),

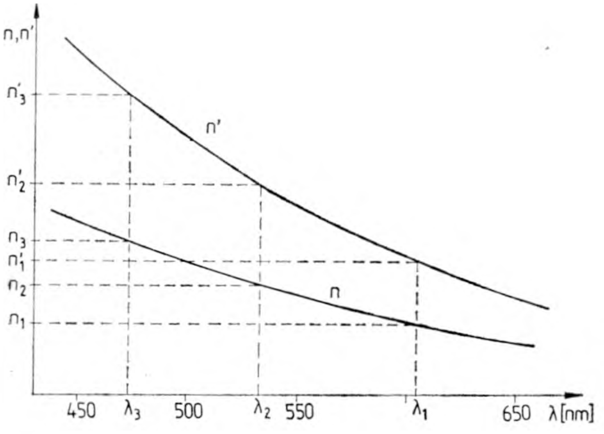

Fig. 1. Typical spectral dispersion curves of the refractive indices of an object under study (n) and its surrounding medium (n')

and that the interference fringes appear in the field of view of the interferometer (Fig. 2). If the optical path difference between the light rays passing through the object and the surrounding medium is greater than the light wavelength,

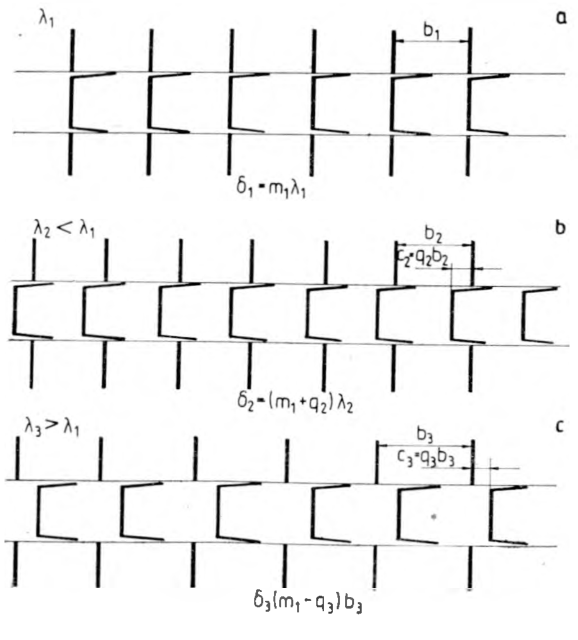

Fig. 2. Illustrating Eq. (1)

then the situation may be described, in general, by the following equations:

$$\delta_1 = (n_1' - n_1)t = m_1 \lambda_1, \tag{1a}$$

$$\delta_2 = (n_2' - n_2)t = (m_1 + q_2)\lambda_2, \tag{1b}$$

$$\delta_3 = (n_3' - n_3)t = (m_1 - q_3)\lambda_3, \tag{1c}$$

where the indices 1, 2 and 3 denote three different wavelengths, δ is the optical path difference, t and n are the thickness and the refractive index of the examined object, respectively, n' is the refractive index of the surrounding medium in which the object is immersed, q is an arbitrary integer or fraction number (Fig. 2), and m_1 is an integer number, called interference order, which in this case is the initial order for the light wavelength λ_1; and $\lambda_2 < \lambda_1$, while $\lambda_3 > \lambda_1$.

From Equations (1a) and (1b) it follows that

$$m_1 = q_2 \frac{\lambda_2}{N_{21}\lambda_1 - \lambda_2} \tag{2}$$

where

$$N_{21} = \frac{n_2' - n_2}{n_1' - n_1}. \tag{3}$$

Similarly, from Equations (1a) and (1c) we have

$$m_1 = q_3 \frac{\lambda_3}{\lambda_3 - N_{31}\lambda_1} \tag{4}$$

where

$$N_{31} = \frac{n_3' - n_3}{n_1' - n_1}. \tag{5}$$

The parameters N_{21} and N_{31} appearing in these formulae may be called factors of similarity of the spectral dispersion of the refractive indices of the object and the surrounding medium. If $n(\lambda) = \text{const}$ and $n'(\lambda) = \text{const}$, $N_{21} = N_{31} = 1$ and the formulae (2) and (4) take a simpler form

$$m_1 = q_2 \frac{\lambda_2}{\lambda_1 - \lambda_2}, \tag{6}$$

$$m_1 = q_3 \frac{\lambda_3}{\lambda_3 - \lambda_1}. \tag{7}$$

The formulae (6) and (7) are valid also when $n(\lambda) \neq \text{const}$, and $n'(\lambda) \neq \text{const}$, but $n'(\lambda) - n(\lambda) = \text{const}$. In this case both the refractive index n of the examined object and the respective index n' of the surrounding medium show spectral dispersion, but all distances between the curves $n(\lambda)$ and $n'(\lambda)$ (Fig. 3) measured in the vertical direction are the same.

From the formulae (1) it follows additionally that

$$N_{21} = \delta_2/\delta_1 \tag{8}$$

and

$$N_{31} = \delta_3/\delta_1. \tag{9}$$

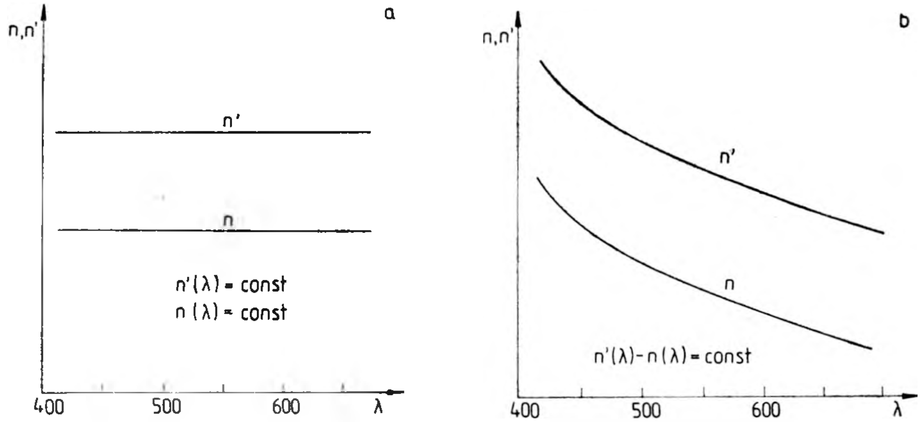

Fig. 3. Illustrating Eqs. (6) and (7)

Therefore, the factors N_{21}, N_{31} may be determined not only from the graphs of the spectral dispersion of refractive indices (comp. Fig. 1), but also from the graph of the spectral dispersion of the optical path difference (Fig. 4). The

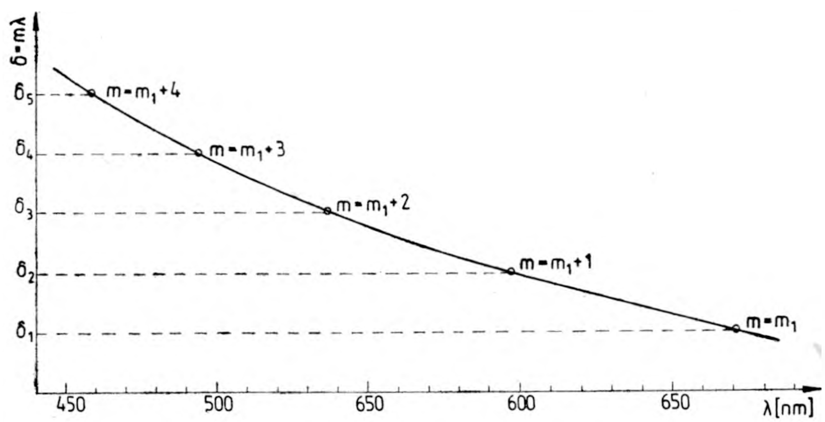

Fig. 4. Optical path difference δ vs. light wevelength λ

latter possibility is of extreme importance in the VAWI method. However, in both the cases the light wavelengths λ_1, λ_2 or λ_3 for which there appears the situation described by Eqs. (1) must be known exactly.

As already mentioned, the parameter q is the integer number or factor expressing simply the increment or decrement of the interference order with respect to m_1 when passing from the wavelength λ_1 to λ_2 or λ_3, respectively. As shown in Fig. 2, $q_2 = c_2/b_2$ or $q_3 = c_3/b_3$, where b_2 and b_3 are the interfringe spacings for the light wavelengths λ_2 and λ_3, while c_2 and c_3 are the displacements of the interference fringes in the image of the examined object, measured from the undeviated fringes with the integer interference order difference equal to m_1. The lesser is the parameter q the smaller the wavelength differences $\lambda_1-\lambda_2$ and $\lambda_3-\lambda_1$. If these differences are small, the coefficients N_{21} and N_{31} in the Eqs. (2) and (4) are practically equal to unity. In this case the formulae (2) and (4) may be replaced by (6) and (7), provided that $q \ll 1$, thus the interference order m_1 may be determined even when the coefficients N_{21} and N_{31} are unknown. This is obvious, especially when the initial interference order m_1 may be chosen in the long-wavelength (red or orange) part of the visible spectrum. Within this spectral range the refractive index dispersion curves of the object and its surrounding medium show a lower and lower slope as λ_1 increases, by the same means the factors N approach closer and closer the unity, when the wavelengths λ_2 and λ_3 differ only slightly from λ_1.

It may be noted, moreover, that if the graphs of the spectral dispersion of the refractive indices n and n' have a run, as shown in Fig. 1. i.e., they tend to diverge in the short-wavelength part of the visible spectrum, then the value m_1 calculated from Eqs. (6) and (7) will be theoretically slightly greater than it

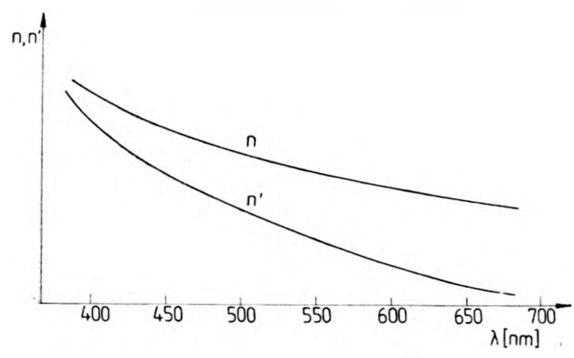

Fig. 5. Refractive index dispersion curves converning in the short-wavelength part of the visible spectrum

follows from Eqs. (2) and (4). If in this case from formulae (6) or (7) it follows, for instance, that $m_1 = 8.6$, then the real order m_1 may be at most equal to 8. Conversely, if the graphs $n(\lambda)$ and $n'(\lambda)$ will tend to converge in the short-wavelength part of the spectral range (Fig 5), the value of m_1 calculated from Eqs. (6) and (7) will be theoretically slightly lower than it follows from Eqs. (2) and (4). If in this case Eq. (6) or (7) gives, for instance, the value $m_1 = 8.4$, then the real order m_1 cannot be smaller than 9.

3. Selection of the most convenient procedure for measuring the optical path difference

As already mentioned, the initial interference order m_1 is most conveniently chosen in the long-wavelength part of the visible spectrum (red or orange). When knowing the order m_1 the optical path difference δ may be measured for arbitrary wavelength λ within the whole visible spectrum range. Depending on the actual object under study more or less convenient measurement situations may occur. If the object introduces significant optical path differences (several times greater than λ), it is convenient to accept the measurement situations following from Eqs. (1a) and (1b), developing the latter into several further equations with the parameter q_2 equal successively to 0.5, 1, 1.5, 2, 2.5 .... Then the following family of equations may be written:

$$\delta_1 = m_1\lambda_1, \tag{10a}$$

$$\delta_2 = (m_1+0.5)\lambda_2, \tag{10b}$$

$$\delta_3 = (m_1+1)\lambda_3, \tag{10c}$$

$$\delta_4 = (m_1+1.5)\lambda_4, \tag{10d}$$

$$\delta_5 = (m_1+2)\lambda_5, \tag{10e}$$

. . . .

. . . .

for $\lambda_1 > \lambda_2 > \lambda_3 > \lambda_4 > \lambda_5 \ldots$, respectively. By changing in a continuous way the light wavelength, the interference fringes deviated by the object under study form with the undeviated ones a collinear structure (Fig. 6a) or pass each other by one half of the interfringe spacing (Fig. 6b). Such positioning of the

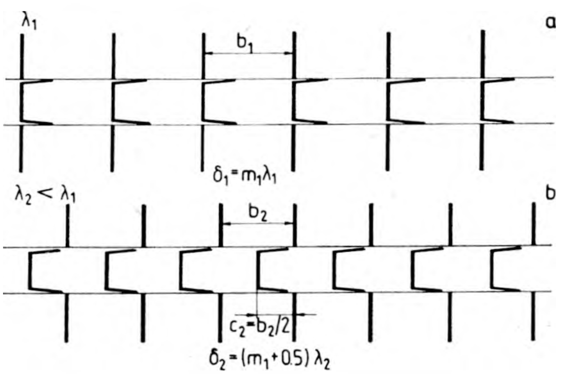

Fig. 6. Illustrating Eqs. (10)

deviated interference fringes with respect to those undeviated may be easily evaluated by the eye without need of measuring the q parameters, since the known vernier principle is applicable. This principle functions especially well, if the object under study is flat and causes no bending of the interference fringes.

If, however, the object is non-flat (e.g., a cylindric fibre), it deforms the fringes in a more or less parabolic way and the vernier principle is perturbed. In this case we can use an ocular supplied with a focal plate with a line indicator according to which the collinear or half-period shifted positions of deviated and undeviated interference fringes are adjusted. It is worth noticing that if a large number of Eqs. (10) is satisfied and the coefficients N are known, or with a good approximation can be accepted to be equal to unity, then the interference order m_1 may be determined from the combination of different pairs of those equations, for instance; from: (10a) and (10b), (10a) and (10c), (10a) and (10d), (10b) and (10c), (10b) and (10d), ... In the opposite case this operation should be limited to two or four first equations referring to the long-wavelength part of the visual spectrum. Thus, in order to determine the initial interference order m_1, it is not always necessary to apply small parameters q and by the same means small differences in the light wavelengths. The acceptance of the parameter $q \ll 1$ requires that the same parameter be measured with a high accuracy, in any case better than $0.01\,\lambda$.

If the object under study introduces a small difference δ of optical path, it may happen that only one measurement possibility with the integer order of interference (m_1) occurs within the whole visible spectrum or even only one half-order ($m_1+0.5$) will appear. In such a case there exists no other choice and m_1 should be determined by measuring small values of parameter q. If Eq. (1a) with integer order (m_1) or half-order of either type ($m_1+0.5$ or $m_1-0.5$) is fulfilled in the middle or within the short-wavelength part of the visible spectrum, the measurement procedure described by Eq. (1b) should rather be rejected using instead Eq. (1c) jointly with Eq. (1a).

4. Additional confirmation of the initial interference order

The first step in the VAWI method is to determine the initial interference order m_1. Next, the optical path difference δ is measured for various light wavelengths in the whole visible spectrum. The interference fringes deviated by the object examined and those undeviated are displaced as the light wavelength λ is changed and the measurement procedure described by Eqs. (10) or by the more general Eqs. (1) are easily observable. The graph of the optical path difference δ is plotted as a function of wavelength λ. When knowing the thickness t of the examined object, the dispersion of the refractive index $n(\lambda)$ may be determined from the graph $\delta(\lambda)$ or vice versa, when knowing $n(\lambda)$ the thickness t may be found if the dispersion $n'(\lambda)$ of the immersion surrounding medium is known in both the cases.

In order to make sure that the initial interference order m_1 has been correctly established the factor

$$N'_{FC} = \frac{\delta_F}{\delta_C} = \frac{n'_F - n_F}{n'_C - n_C} \tag{11}$$

should be analysed (here F and C denote the spectral lines of wavelengths $\lambda_F = 486$ nm and $\lambda_C = 656$ nm). If the interference order m_1 is wrongly accepted and differs from the real one by $+1$ or -1, then the factor N'_{FC} will differ incredibly from that characterizing the known dielectric substances of normal dispersion of the refractive index. The factor N'_{FC} is obviously read out from the graph of $\delta(\lambda)$ made before.

Thin films, fibres, stripes of foil, plate-like microcrystals and other solid preparations may be measured at best (if possible) in the air medium. In such conditions the VAWI method is especially suitable for interferometry. Thus, if the air plays the part of an immersion surrounding medium, then in Eqs. (1)–(10) n' should be assumed to be equal to unity. In such a situation the formula (11) takes the form

$$N_{FC} = \frac{\delta_F}{\delta_C} = \frac{n_F - 1}{n_C - 1}. \tag{12}$$

In Table 1 the values of the factor N_{FC} are given for several characteristic substances of refractive index n_D contained within the 1.5–2.4 interval. It

Table 1. Dispersion factors N_{FC} of some characteristics substances transparent in visible spectrum

Substance	Refractive indices			$N_{FC} = \dfrac{n_F - 1}{n_C - 1}$
	n_D	n_F	n_C	
Water	1.3330	1.3377	1.3312	1.0196
Optical glass FK3	1.4645	1.4694	1.4623	1.0153
Zeiss refractometric plate	1.5133	1.5170	1.5090	1.0157
Immersion oil	1.5169	1.5256	1.5135	1.0236
Optical glass F2	1.6241	1.6321	1.6150	1.0278
Carbon disulphide	1.6277	1.6523	1.6181	1.0553
Optical glass SF10	1.7283	1.7465	1.7208	1.0357
Optical glass SF6	1.8052	1.8277	1.7961	1.0397
Optical glass SFS1	1.9229	1.9545	1.9104	1.0484
Cargille hight dispersion liquids:	1.500	1.5134	1.4943	1.0386
	1.550	1.5664	1.5437	1.0418
	1.600	1.6196	1.5924	1.0459
	1.650	1.6718	1.6416	1.0471
	1.700	1.7263	1.6898	1.0529
	1.750	1.7775	1.7393	1.0517
	1.800	1.8361	1.7850	1.0651
Poly(p-phenylene terephthalamide) fibre $n_\parallel$	2.360	2.455	2.335	1.0899

should be noted that the criterion (12) is much stronger than (11). This is an additional argument justifying what was said above that VAWI method is especially suitable to the interference measurements carried out in the air medium. Obviously, this constitutes its essential merit.

5. Measuring examples by using the double refracting interference microscope (Biolar PI)

The VAWI method – as already mentioned in the Introduction – is especially suitable to be used jointly with the double-refracting interference microscope Biolar PI (Fig. 7). This microscope offers an important advantage of making possible a current measurement of the wavelength of the monochromatic light entering its interference system.

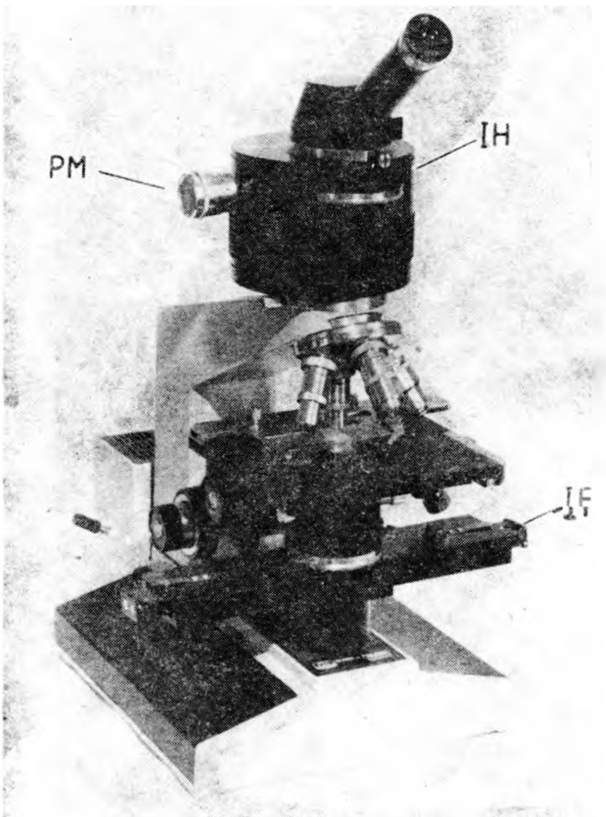

Fig. 7. Biolar PI double-refracting interference microscope. IH – interference head, PM – micrometric phase screw, IF – interference monochromator (wedge interference filter)

There exists a rigorous and constant relation between the interfringe distance b of the fringe interference field and the value of the wavelength λ [4]. This relation is of an almost linear character in the visible spectrum range (Fig. 8) and the graph of $b(\lambda)$ may be considered as a basic gauging of the Biolar PI interference microscope system. This procedure must be carried out very carefully by using highly monochromatic light, for instance, the light from lasers of several standard wavelengths, and is performed only once. The once plotted graph of $b(\lambda)$ is valid for ever. By assuming a linear relation between b and λ, which is true to a high degree [4], the formulae (2) and (4) may be written in the form

$$m_1 = q_2 \frac{b_2}{N_{21}b_1 - b_2}, \tag{13}$$

$$m_1 = q_3 \frac{b_3}{b_3 - N_{31}b_1}. \tag{14}$$

Similarly, the formulae (6) and (7) may be expressed as

$$m_1 = q \frac{b_2}{b_1 - b_2}, \tag{15}$$

$$m_1 = q \frac{b_3}{b_3 - b_1}. \tag{16}$$

A continuous linear interference filter (IF, Fig. 7) may be used effectively together with the Biolar PI microscope to vary continuously the light wavelength in the VAWI method. This filter is placed immediately in front of the polarizer

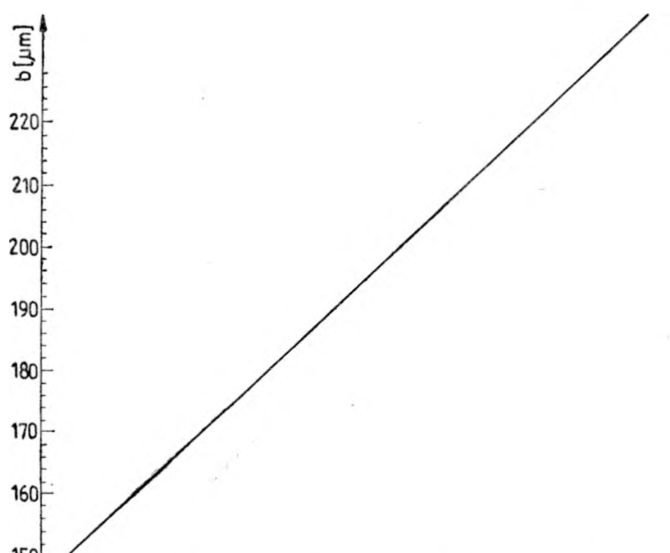

Fig. 8. Dependence between the interfringe spacing b and light wavelength λ for the birefringent prism No. 2 of the Biolar PI microscope

positioned in the neighbourhood of the condenser slit diaphragm of the Biolar PI microscope. Since the latter makes it possible – as already mentioned – to measure currently the peak wavelength of light transmitted through the subsequent narrow segments of the filter limited by the condenser diaphragm slit, the filter need not be calibrated and supplied with a suitable wavelength scale. The procedure leading to the current determination of the local peak wavelength of the filter may be found in the paper [4]. It consists simply in the measurement of the distance b between the interference fringes produced by the light of the given wavelength. This measurement is carried out with the help of the micrometer screw PM, called phase screw, which is associated with the transversal displacement of the birefringent prism No. 2 in the interference head of the Biolar PI microscope. The displacement of the prism is accompanied with the movement of the interference fringes in the field of view of the microscope; the latter is provided with an ocular with a line indicator on which the centres of the fringes are guided. In this case by measuring an interfringe distance multiple, for instance, ten distances, between the fringes of plus and minus fifth interference order rather than a single interfringe distance, a more accurate determination of b is achieved. When knowing the interfringe distance b the wavelength λ is read out from the graph of $b(\lambda)$ plotted earlier (Fig. 8).

First measurement example. The tests were performed on some gradient refractometric plates made of the optical FK3 and F2 glasses of nominal refractive indices $n_d = 1.4645$ and $n_d = 1.6200$, respectively. The graphs of the refractive index vs. the light wavelength are presented in Fig. 9. These plates

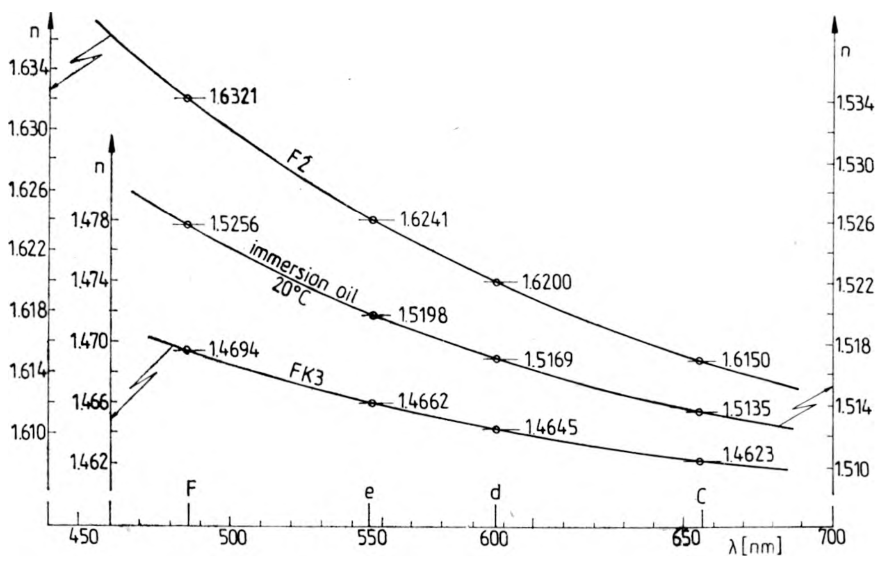

Fig. 9. Refractive index dispersion curves for the FK3 and F2 refractometric plates, and that for the Cargille immersion oil

belonging to additional equipment of Biolar PI microscope) were immersed in an immersion oil of refractive index $n_D = 1.5169$ (at 20°C temperature). The difference between the refractive index of the immersion oil and that of the refractometric plates was so small that the process of connection of the deviated and undeviated fringes was easily observed (Fig. 10). The interference orders were thus easily identifiable visually, while the main idea of the experiment was to state whether the initial interference order observed in the red light is identical with the order following from Eqs. (10). The results are presented in Tables 2 and 3. As can easily be seen, the consistence between the observed order m_1 and that following from Eqs. (10) is very high. For the FK3 plate the order $m_1 = 3$ was observed in the red part of the spectrum, while the average value following from Eqs. (10) was $m_1 = 3.02$, i.e., also $m_1 = 3$. Similar agreement was observed in the second case (F2 refractometric plate): $m_1 = 5$ in the yellow light, and computed from Eqs. (10) $m_1 = 5.07$, i.e., also $m_1 = 5$.

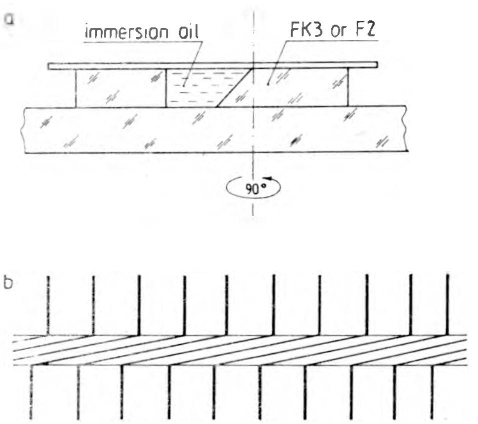

Fig. 10. Interference image (b) of the measuring region of the gradient refractometric plate (a) observed through the Biolar PI microscope

Table 2. Results of the experiment with the FK3 gradient refractometric plate ($n_d = 1.4645$)

Measuring situation s	1	2	3	4	5
Factor q	0	0.5	1	1.5	2
10 b [μm]	2192.0	1914.5	1728.5	1577.0	1460.0
λ [nm]	633.0	559.5	509.5	470.0	439.0
n	1.4629	1.4656	1.4680	1.4705	1.4728
n'	1.5149	1.5192	1.5236	1.5281	1.5328
$\Delta n = n' - n$	0.0520	0.0536	0.556	0.0576	0.0600
N_{s1}	1	1.0308	1.0692	1.1077	1.1539
N_{s2}	0.9702	1	1.0373	1.0746	1.1194
N_{s3}	0.9353	0.9640	1	1.0360	1.0791
N_{s4}	0.9028	0.9306	0.9653	1	1.0417
N_{s5}	0.8667	0.8933	0.9267	0.9600	1
m_1 (N_{s1}, λ)	—	3.01	3.05	3.05	3.01
m_1 (N_{s2}, λ)	3.01	—	3.09	3.08	3.02
m_1 (N_{s3}, λ)	3.05	3.09	—	3.06	2.96
m_1 (N_{s4}, λ)	3.05	3.08	3.06	—	2.84
m_1 (N_{s5}, λ)	3.01	3.02	2.96	2.84	—
Mean value $\overline{m}_1$ (N_{ss}, λ)	3.03	3.05	3.04	3.01	2.96
Resultant mean value $\overline{m}_1 = 3.02$, hence it appears that $m_1 = 3$					
m_1 (λ_{s1})	—	3.8	4.1	4.3	4.5
m_1 (λ_{s2})	3.8	—	4.6	4.7	4.9

Table 3. Results of the experiment with the F3 gradient refractometric plate ($n_d = 1.6200$)

Measuring situation s	1	2	3	4	5
Factor q	-0.5	0	0.5	1	1.5
$10b$ [μm]	2218.5	2010.0	1838.0	1706.0	1578.0
λ [nm]	640.0	585.0	539.0	504.0	470.5
n	1.6160	1.6203	1.6249	1.6294	1.6349
n'	1.5140	1.5169	1.5201	1.5232	1.5269
$\Delta n = n - n'$	0.1020	0.1034	0.1048	0.1062	0.1080
N_{s1}	1	1.0137	1.0275	1.0412	1.0588
N_{s2}	0.9865	1	1.0135	1.0271	1.0445
N_{s3}	0.9733	0.9866	1	1.0134	1.0305
N_{s4}	0.9605	0.9736	0.9868	1	1.0170
N_{s5}	0.9444	0.9574	0.9704	0.9833	1
m_1 (N_{s1}, λ)	—	5.09	5.05	5.16	5.04
m_1 (N_{s2}, λ)	5.09	—	5.00	5.20	5.20
m_1 (N_{s3}, λ)	5.05	5.00	—	5.47	5.04
m_1 (N_{s4}, λ)	5.16	5.20	5.47	—	4.60
m_1 (N_{s5}, λ)	5.04	5.02	5.04	4.60	—
Mean value $\overline{m}_1$ (N_{ss}, λ)	5.09	5.08	5.14	5.11	4.93
Resultant mean value $\overline{m}_1 = 5.07$, hence it appears that $m_1 = 5$					
m_1 (λ_{s1})	—	5.8	5.8	6.1	6.1
m_1 (λ_{s2})	5.8	—	5.9	6.2	6.2

The same values are obtained if the dispersive factors N in the formulae are taken to be equal to unity. Thus, for example, in the first case (FK3 plate) m_1 calculated from Eqs. (10a) and (10b) is equal to 3.8. Keeping in mind what has been said formerly at the final part of Sec 2 we may assume that in this case m_1 is at most equal to 3. Analogically, in the second case (F2 plate) the value m_1 estimated from Egs. (10a) and (10b) is $m_1 = 5.8$. This means that m_1 may be at most equal to 5.

In Figure 11 the graphs of the optical path difference δ vs. the light wavelength λ are shown for the system: FK3 refractometric plate + immersion oil, under assumptions that $m_1 = 3$ (graph 1), $m_1 = 2$ (graph 2), and $m_1 = 4$ (graph 3). From graph 1 it follows that the factor $N'_{FC}(3) = 1.1005$, while from graphs 2 and 3 we have $N'_{FC}(2) = 1.2874$ and $N'_{FC}(4) = 1.0098$. The value of $N'_{FC}(3)$ is within the measurement error consistent with that following from Fig. 9. On the other hand, the values of factor $N'_{FC}(2)$ and $N'_{FC}(4)$, as well as graphs 2 and 3 are nonrealistic; confirm therefore additionally that the initial interference order $m_1 = 3$.

Similar graphs for the system F2 refractometric plate + immersion oil are presented in Fig. 12 under assumptions that $m_1 = 5$ (graph 1), $m_1 = 4$ (graph 2), and $m_1 = 6$ (graph 3). From the first graph it follows that $N'_{FC}(5) = 1.059$, from the second – $N'_{FC}(4) = 1.149$ and from the third – $N'_{FC} = 1.0014$. The first value is consistent with that following from Fig 9, while the others are unreal.

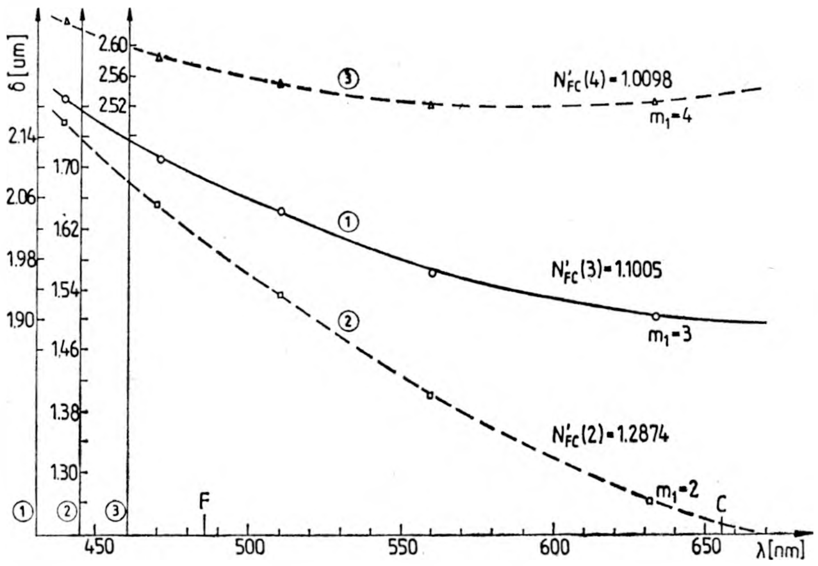

Fig. 11. Experimental graphs of the spectral dispersion of the optical path difference δ for the system: FK3 refractometric plate + immersion oil, under assumption that the initial interference order $m_1 = 3$ (graph 1), $m_1 = 2$ (graph 2), and $m_1 = 4$ (graph 3)

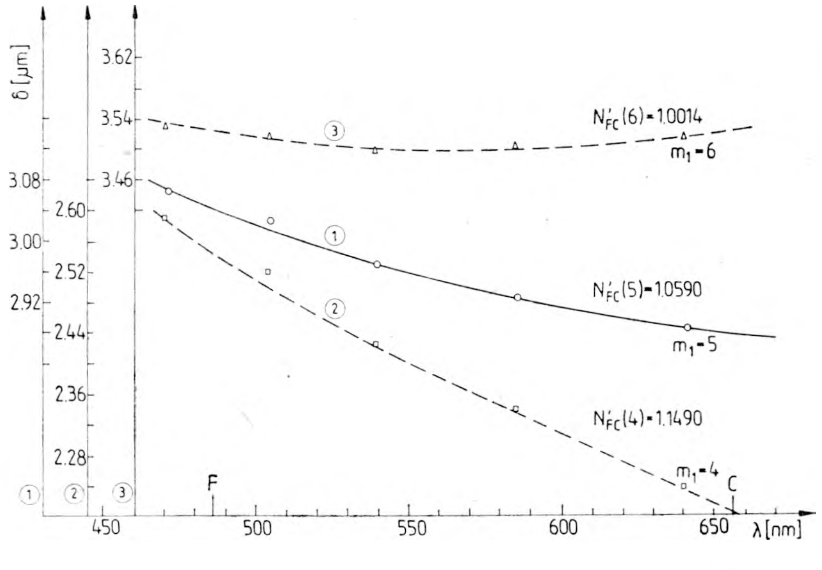

Fig. 12. As in Fig. 11, but for the system: F2 refractometric plate + immersion oil, under assumption that the initial interference order $m_1 = 5$ (graph 1), $m_1 = 4$ (graph 2), and $m_1 = 6$ (graph 3)

Thus, also in this case, the above analysis confirms additionally that the initial interference order is equal to five.

The nonrealistic character of graphs 3 in Figs. 11 and 12 follows from the fact that, contrary to the experimental observations, they indicate an almost constant optical path difference in the whole range of the visual spectrum and thus a constant difference $\Delta n(\lambda)$ of the refractive indices of the immersion oil and the refractometric plate, whereas the fictitious character of the graphs 2 follows from the indication of an exaggeratedly high spectral dispersion of the $\Delta n(\lambda)$ which was never observed.

Second measurement example. In the second experiment the measurements concerned the depth t of a groove in the Zeiss refractometric plate which was fixed by the producer to be $t = 10.0230$ μm (Fig. 13). The graph of dispersion

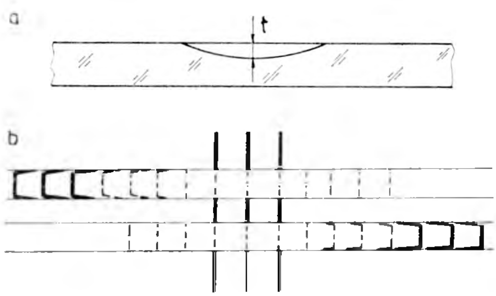

Fig. 13. Interference image (b) of the measuring region of the Zeiss refractometric plate (a), observed through the Biolar PI microscope

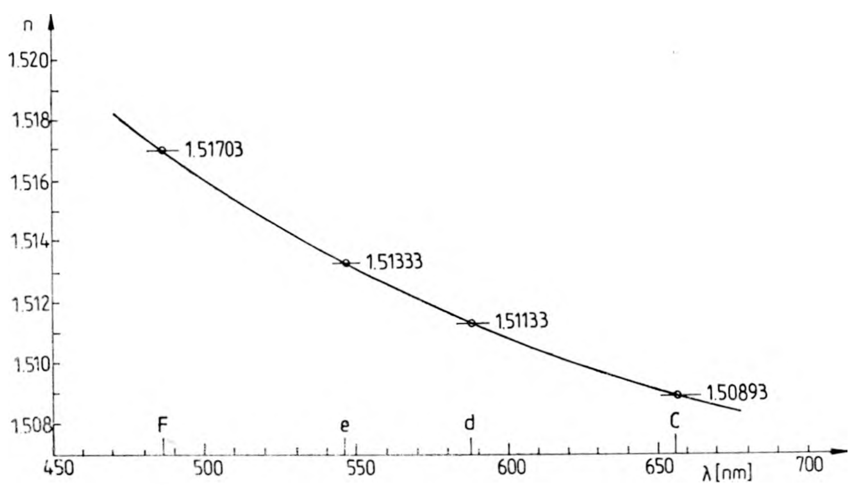

Fig. 14. Spectral dispersion of the refractive index of the Zeiss refractometric plate (factory number 620575)

$n(\lambda)$ for this plate (made after the producer's data) is shown in Fig. 14. In the transmitted light and in the air surrounding medium the deflection of the interference fringes due to the said groove was so high that no connections of the deflected fringes with those undeflected were seen (Fig. 13b). Therefore, first of all the interference order m_1 had to be identified by using the VAWI method. The measurement procedure was, in general, determined by the first seven Eqs. (10). The measured interfringe distence b, the light wavelength read from the graph $b(\lambda)$ – Fig. 8, the dispersive factors N following from the graph $n(\lambda)$ – Fig. 14, and the initial interference order m_1 calculated from all possible combinations of two different formulae of the equation system (10) are given in Table 4. It has been stated that $m_1 = 8$ for the wavelength $\lambda_1 = 635.5$ nm. Next, for the wavelengths $\lambda_1, \lambda_2, \lambda_3, \ldots$ optical path differences δ satisfying seven first equations of the system (11) were calculated and the groove depth t was determined. Averaging the individual results yielded $t = 9.990$ μm differing only by 0.033 μm from the value given by the producer of the refractometric plate.

Table 4. Results of the experiment with the Zeiss refractometric plate whose groove depth t = 10.0230 μm (after the manufacturer's data)

Measuring situation s	1	2	3	4	5	6	7
Factor q	0	0.5	1	1.5	2	2.5	3
10b [μm]	2200.0	2066.0	1951.0	1841.5	1742.5	1663.5	1578.5
λ [nm]	635.5	599.5	569.0	540.0	513.5	493.0	471.0
n	1.5096	1.5108	1.5121	1.5136	1.5152	1.5165	1.5182
n'	1	1	1	1	1	1	1
$\Delta n = n - n'$	0.5096	0.5108	0.5121	0.5136	0.5152	0.5165	0.5182
N_{s1}	1	1.0024	1.0049	1.0079	1.0110	1.0135	1.0168
N_{s2}	0.9977	1	1.0026	1.0055	1.0086	1.0112	1.0144
N_{s3}	0.9951	0.9975	1	1.0029	1.0061	1.0086	1.0119
N_{s4}	0.9922	0.9946	0.9971	1	1.0031	1.0057	1.0089
N_{s5}	0.9891	0.9915	0.9940	0.9969	1	1.0025	1.0058
N_{s6}	0.9866	0.9890	0.9915	0.9944	0.9975	1	1.0033
N_{s7}	0.9834	0.9857	0.9882	0.9911	0.9942	0.9967	1
m_1 (N_{s1}, λ)	—	7.99	8.17	8.06	7.96	8.16	8.06
m_1 (N_{s2}, λ)	7.99	—	8.38	8.10	7.95	9.21	8.08
m_1 (N_{s3}, λ)	8.17	8.38	—	7.80	7.71	8.14	7.99
m_1 (N_{s4}, λ)	8.06	8.10	7.80	—	7.61	8.35	8.07
m_1 (N_{s5}, λ)	7.96	7.95	7.71	7.61	—	×	8.35
m_1 (N_{s6}, λ)	8.16	8.21	8.14	8.35	×	—	7.47
m_1 (N_{s7}, λ)	8.06	8.08	7.99	8.07	8.35	7.47	—
Mean value $\overline{m}_1$ (N_{ss}, λ)	8.07	8.12	8.03	8.00	7.92	8.07	8.00
Resultant mean value $\overline{m}_1$ = 8.03, hence it appears that $m_1 = 8$							
Interference orders m_s	8 (= m_1)	8.5	9	9.5	10	10.5	11
$\delta = m_s \lambda$ [μm]	5.0840	5.0958	5.1210	5.1300	5.1350	5.1765	5.1810
$t = \delta/\Delta n$ [μm]	9.9765	9.9760	10.0000	9.9883	9.9670	10.0223	9.9981
Mean value of the groove depth $\bar{t}$ = 9.990 μm							

In order to make sure completely whether the initial interference order has been determined correctly, the graphs $\delta(\lambda)$ have been made assuming that $m_1 = 8$ (graph 1 in Fig. 15), $m_1 = 7$ (graph 2) and $m_1 = 9$ (graph 3). As can easily be seen both graphs 2, 3 and the factors $N_{FC}(7)$, $N_{FC}(9)$ are highly improbable. From graph 3 it follows that the refractive index of the refractometric plate should increase with the light wavelength which, in this case, would be a nonsense, while factor $N_{FC}(7)$ resulting from graph 2 is as high as that characteristic of substances of nominal refractive index $n_D = 1.75$ (comp. Tab. 1). Therefore, the initial interference order may be neither 7 nor 9, but solely 8.

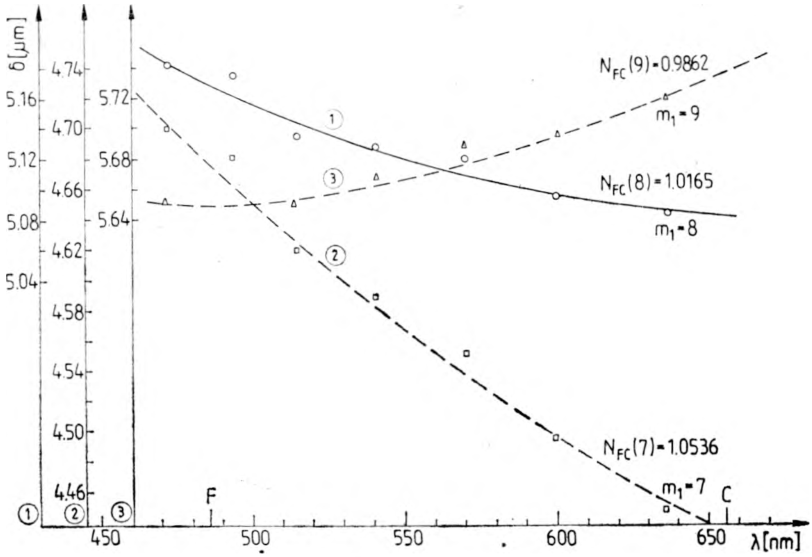

Fig. 15. Experimental graphs of the spectral dispersion of the optical path difference δ due to the groove of the Zeiss refractometric plate, under assumption that the initial interference order $m_1 = 8$ (graph 1), $m_1 = 7$ (graph 2), and $m_1 = 9$ (graph 3)

Third measurement example. The groove of the refractometric plate has been filled with water distilled and covered with a microscope cover glass. The purpose of the experiment was to determine the dispersion $n'(\lambda)$ of water. The results are shown in Table 5 and in Fig. 16. Graph 1 is referred to the groove depth $t = 9.99$ μm which has been determined in the second experiment, while graph 2 – to the depth $t = 10.023$ μm reported by the producer. As can easily be seen, the difference $\Delta t = 0.033$ μm causes the difference $\Delta n' \approx 0.0005$. The measurements were made at the ambient temperature of 21°C. The graph of water dispersion according to the literature data for 20°C, given for comparative reasons, is plotted with a broken line. In view of the fact that when the temperature increases by 1°C the water refractive index slightly decreases, the assumption that $t = 9.99$ μm gives the more reliable result of measurement, since by assuming the depth of refractometric plate groove, as reported by the producer slightly higher values of n' are obtained. The difference $\Delta n'$ is really negligeable and this experiment together with the previous one give a convincing evidence about the advantages offered by the VAWI method.

6. Conclusions

The cited experimental results have confirmed the general correctness of the new interferometric method and indicated its practical value, especially when high optical path differences, significantly greater than the light wavelength, are to be measured. Such situations occur in practice very often, especially

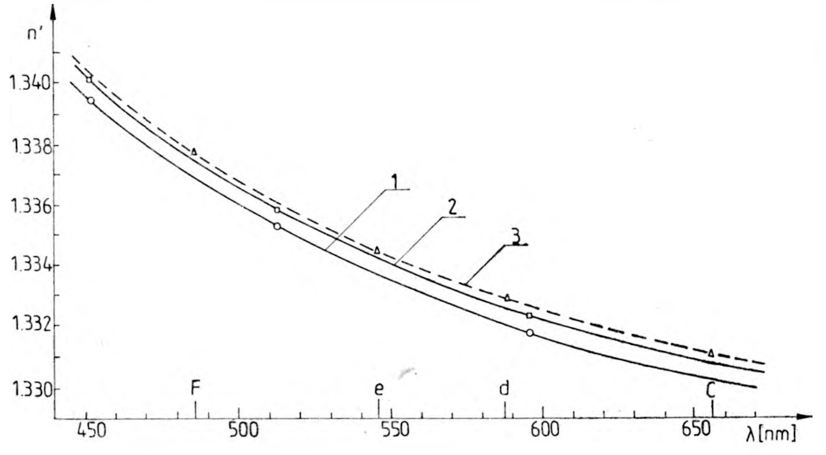

Fig. 16. Graphs of the spectral dispersion of the refractive index n' of the distilled water, at 21°C, under assumption that the groove depth t of the Zeiss refractrometric plate is equal to 9.99 μm (graph 1) and $t = 10.023$ μm (graph 2). The broken curve 3 represents the refractive index dispersion of the distilled water according to the literature data (at 20°C)

Table 5. Results of the measurement of the spectral dispersion of the refractive index (n') of the distilled water by using the Zeiss refractometric plate (at 21°C)

Measuring situation s	1	2	3
Factor q	0	0.5	1
$10b$ [μm]	2051.8	1742.0	1505.4
λ [nm]	596.0	513.5	451.5
Refractive index n of the plate	1.5109	1.5152	1.5203
m_{1s} (from Eq. (6))	—	3.11	3.11
Interference orders m_s	$3(=m_1)$	3.5	4
$\delta = m_s\lambda$ [μm]	1.7880	1.7973	1.8060
$n-n' = \delta/t = \delta/9.99$	0.1790	0.1799	0.1808
n'	1.3319	1.3353	1.3395
$n-n' = \delta/t = \delta/10.023$	0.1784	0.1793	0.1802
n'	1.3325	1.3359	1.3401

when the examined object is surrounded by the air or, for some reasons, it cannot be located in the immersion liquid in order to diminish the optical path difference. The VAWI method is suitable also for measurement of thin objects providing small optical path differences, but in the uniform interference version (the interference fringes are infinitely extended in the field of view). This problem will be the subject of another paper.

The main advantage offered by the VAWI method is that it allows us to identify the interference orders when the interference fringes deflected by the object under study show no perceivable connections with the undeviated fringes.

Another advantage of the VAWI method is that it enables a relatively quick measurement of the optical path differences within the whole visible spectrum, which is especially important for measurements of the spectral dispersion of the refractive index. When having the graph $\delta(\lambda)$ a more accurate value of δ or n may be obtained for a given light wavelength by smoothing the graph, than by performing a single-wavelength measurement.

The measurement procedure in the VAWI method is simple and relatively quick. The procedure described by Eqs. (11) is reduced to the measurement of the interfringe distance b and this measurement may be made extraordinarily accurate, since in a sufficiently monochromatic light a multiple (for instance, ten times greater) value of b can be measured.

The WAVI method may be especially useful for the measurement of birefringence of textile fibres, especially of those characterized by a high degree of extension. The fibre examined must not be immersed in an immersion liquid as it is practiced in the traditional microinterferometric procedures. This is a very important advantage offered by the VAWI method, since almost always the immersion liquid changes more or less the optical and geometrical properties of the textile fibre. Another paper will be devoted to the last topic.

References

[1] Pluta M., *Abstracts of the European Optical Conference (EOC'-83)*, May 30–June 4, 1983, Rydzyna, p. 131.
[2] Pluta M., J. Phys. E. (Sci. Instrum.) **2** (1969), 685–690.
[3] Pluta M., Optica Acta **18** (1971), 661–675.
[4] Pluta M., Optica Applicata **12** (1982), 19–36.

Received March 6, 1985

Интерферометрия с плавно переменной длиной волны. I. Полосатый метод для проходящего света

Разработан новый метод измерения разности оптического пути во всем диапазоне видимого спектра. В этом методе используется монохроматический свет с плавно переменной длиной волны. Простой способ идентифицирования ряда интерференционных полос это одна из главных примет этого метода. Разработанный метод особенно хорошо взаимодействует с двоякопреломляющим интерференционным микроскопом Biolar PI потому что этот микроскоп позволяет измерить длину монохроматического света в текущее время.